



AFGL-TR-81-0357

ATMOSPHERIC TRANSMITTANCE/RADIANCE  
COMPUTER CODE FASCOD2

W.L. RIDGWAY  
R.A. MOOSE  
A.C. COGLEY

SONICRAFT, INC.  
8859 S. GREENWOOD AVENUE  
CHICAGO, ILLINOIS 60619

16 OCTOBER 1981

Scientific Report No. 2

Approved for public release; distribution unlimited

Prepared for:

AIR FORCE GEOPHYSICS LABORATORY  
AIR FORCE SYSTEMS COMMAND  
UNITED STATES AIR FORCE  
HANCOM AFB, MASSACHUSETTS 01751

DTIC  
SELECTED  
APR 27 1982  
H

82 04 27 181

AD A113825

Qualified requestors may obtain additional copies from the  
Defense Technical Information Center. All others should  
apply to the National Technical Information Service.

UNCLASSIFIED

SECURITY CLASSIFICATION OF THIS PAGE (When Data Entered)

REPORT DOCUMENTATION PAGE		READ INSTRUCTIONS BEFORE COMPLETING FORM
1. REPORT NUMBER AFGL-TR-81-0357	2. GOVT ACCESSION NO. AD A113 825	3. REPORT'S CATALOG NUMBER
4. TITLE (and Subtitle) ATMOSPHERIC TRANSMITTANCE/RADIANCE COMPUTER CODE FASCOD2	5. TYPE OF REPORT & PERIOD COVERED Scientific Report No.2	
	6. PERFORMING ORG. REPORT NUMBER	
7. AUTHOR(s) W.L. Ridgway R.A. Moose A.C. Cogley	8. CONTRACT OR GRANT NUMBER(s)  F19628-79-C-0120	
9. PERFORMING ORGANIZATION NAME AND ADDRESS Sonicraft, Inc. 8859 S. Greenwood Avenue Chicago, Illinois 60619	10. PROGRAM ELEMENT, PROJECT, TASK AREA & WORK UNIT NUMBERS  62101 F 767009AM	
11. CONTROLLING OFFICE NAME AND ADDRESS Air Force Geophysics Laboratory Hanscom AFB, Massachusetts 01731 Monitor/Francis X. Kneizys/OPI	12. REPORT DATE 16 October 1981	
	13. NUMBER OF PAGES 38	
14. MONITORING AGENCY NAME & ADDRESS (if different from Controlling Office)	15. SECURITY CLASS. (of this report)  Unclassified	
	15a. DECLASSIFICATION/DOWNGRADING SCHEDULE	
16. DISTRIBUTION STATEMENT (of this Report)  Approved for public release; distribution unlimited		
17. DISTRIBUTION STATEMENT (of the abstract entered in Block 20, if different from Report)		
18. SUPPLEMENTARY NOTES		
19. KEY WORDS (Continue on reverse side if necessary and identify by block number)		
Radiative transfer	Non-equilibrium	CO <sub>2</sub> continuum
Layered atmosphere	Non-LTE	CO <sub>2</sub> line wings
Atmospheric transmittance	Lineshape profiles	
Atmospheric radiance	Lorentz profile	
20. ABSTRACT (Continue on reverse side if necessary and identify by block number)		
<p>✓ Modifications to the fast line-by-line atmospheric transmittance and radiance code FASCOD1B are detailed. CO<sub>2</sub> far wings are modelled with a new sub-Lorentz lineshape which more properly accounts for foreign gas broadening. A two-parameter exponential-type form factor is developed and used for this purpose. The problem of radiative transfer in the daylight, non-LTE, upper atmosphere is addressed and a model for radiance and transmittance in such a medium is now incorporated in FASCOD2.</p>		

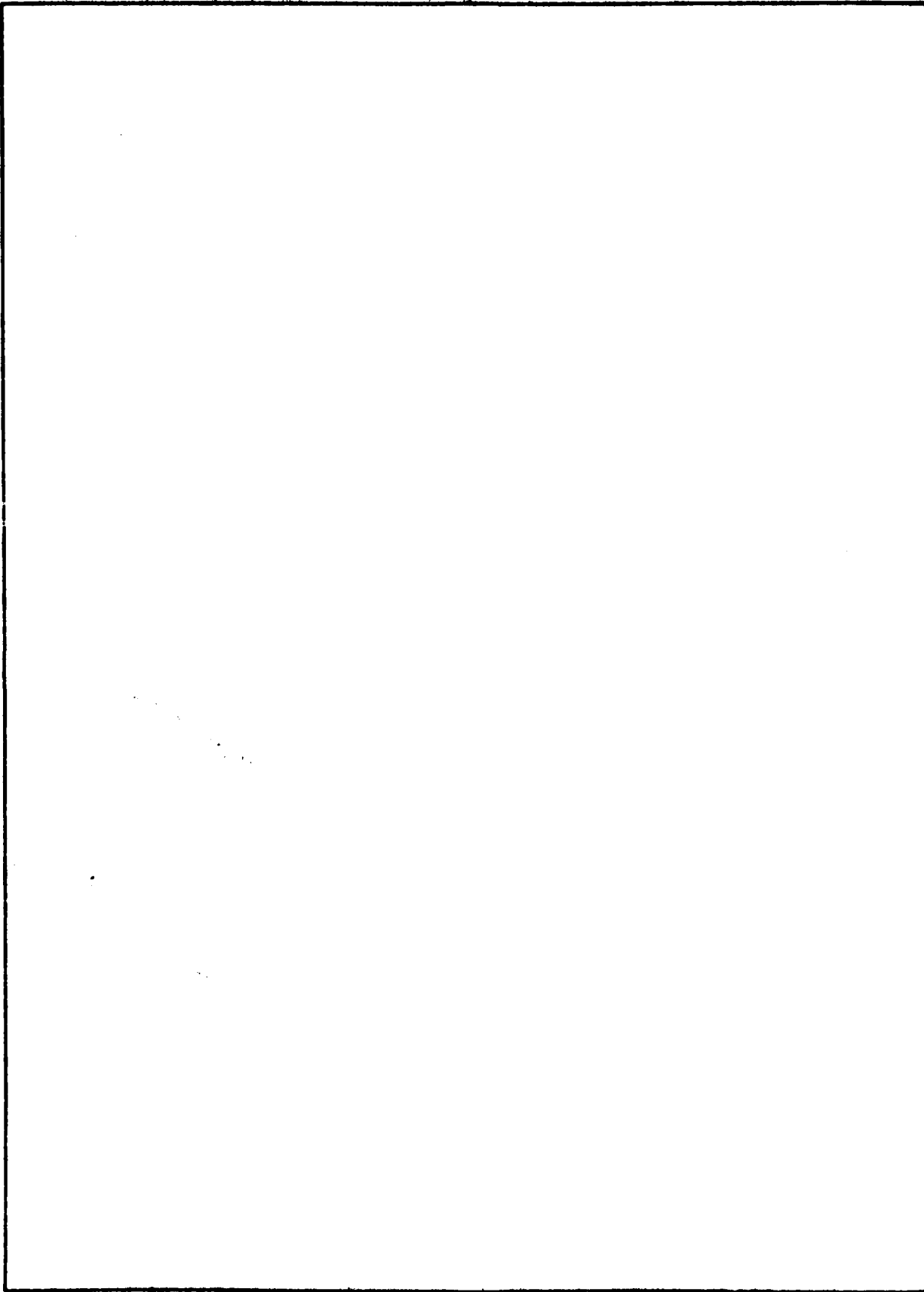
**DTIC  
SELECTED  
APR 27 1982  
S H D**

DD FORM 1 JAN 73 1473 EDITION OF 1 NOV 65 IS OBSOLETE

UNCLASSIFIED

SECURITY CLASSIFICATION OF THIS PAGE (When Data Entered)

SECURITY CLASSIFICATION OF THIS PAGE(When Data Entered)



SECURITY CLASSIFICATION OF THIS PAGE(When Data Entered)

TABLE OF CONTENTS

SECTION	PAGE
1. Introduction .....	5
2. CO <sub>2</sub> Continuum Absorption and FASCODE Lineshape Models .....	7
3. Non-LTE Radiance and Transmittance Calculations .....	20
4. Lineshape Control Features and Program Structure Changes .....	31
5. Summary .....	36
References .....	37

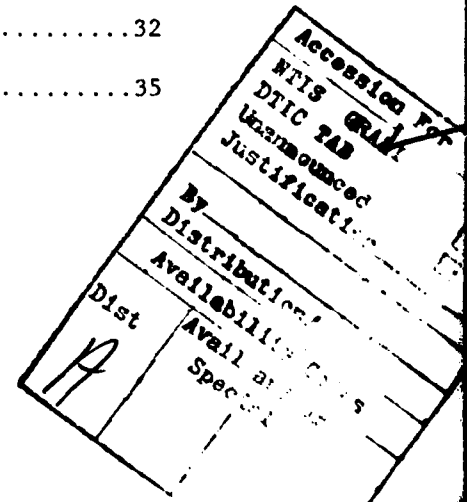
LIST OF FIGURES AND TABLES

FIGURE

1. Comparision of Sample FASCODE CO <sub>2</sub> Transmittance to other Simulations.....	19
2. Radiance in Units of Equivalent Blackbody Temperature for a 500 km Path at 100 km Altitude Assuming LTE and Non-LTE Vibrational Populations .....	30

TABLE

1. FASCODE Lorentz Lineshape Subfunctions .....	11
2. Comparision of Various CO <sub>2</sub> Lineshape Form Factors .....	15
3. Routines Used to Produce the CO <sub>2</sub> Lineshape .....	32
4. Non-LTE Routines .....	35



## 1. INTRODUCTION

This report continues the process, begun in the first FASCOD2 report [Ref.1], of describing the work completed and in progress on the development of a computer code called FASCOD2 that efficiently calculates high spectral resolution transmittance and radiance in the earth's atmosphere. The present code has evolved from earlier versions designated FASCODE [Ref.2] and FASCOD1B [Ref.3]. The prior report [Ref.1] documented the modifications required to use the newer AFGL geometry [Ref.4] routine for a spherically layered refractive medium and to incorporate the atmospheric data base found in the current LOWTRAN 5 code [Ref.5]. Zeroth order aerosol scattering and absorption, as modelled by LOWTRAN 5, were also included in FASCOD2. This restructuring of the code was completed and documented in the previous report.

Reference 1 discussed the problem of characterizing the continuum absorption caused by the far wings of the many overlapped CO<sub>2</sub> lines near a band head. Section 2 completes this research topic and documents the changes made to FASCOD2 to include this phenomenon. The far-wing CO<sub>2</sub> lineshape is made sub-Lorentzian by a simple parametric multiplication function. However, the parameters are obtained by fitting laboratory absorption data. Selected results from this new version of FASCOD2 are presented and compared with other available predictions and observations.

At the higher altitudes the photo-driven chemistry and reduced molecular collision rate can make the usual assumption of local thermodynamic equilibrium (LTE) incorrect. Degges and Smith [Ref.6] have modelled such phenomena for certain selected vibrational transitions and have predicted non-LTE population densities for certain atmospheric conditions, i.e., daylight, night, and selected season (sun angle). The first report outlined a model for non-LTE radiative transfer compatible with FASCOD2's structure and this work is now completed in Section 3. Code changes are documented and sample computational results are presented to show the change in radiance caused by non-LTE effects using the output from Degges' calculations.

Section 4 gives an outline of the subprograms added or modified in FASCOD2 to accomplish the work described in Sections 2 and 3. The remaining tasks on FASCOD2 are summarized in Section 5.

## 2. CO<sub>2</sub> CONTINUUM ABSORPTION AND FASCODE LINESHAPE MODELS

The line-by-line HIRACC algorithm [Ref.7] has been extended to include the lineshape region within 256 halfwidths of line center of each spectral line [Refs.2,3]. The primary consideration in extending the lineshape bound from 64 halfwidths was to fit the band edge, and region of continuum absorption which is thought to arise primarily from the cumulative contribution from the wings of many overlapping lines. The continuum absorption is known to scale linearly with both the gas amount and the broadening gas density (more precisely, the molecular collision frequency) in the high pressure (Lorentz shape) limit [Refs.8,9], and can thus be modelled by scaling a continuum function defined at a reference pressure and temperature which is obtained from laboratory measurements. The process is complicated if multiple broadening mechanisms must be accounted for, as in the case of self and foreign gas broadening of water vapor lines. This problem has been the focus of work at AFGL and is discussed in a previous report [Ref.3].

In order to model the CO<sub>2</sub> continuum at typical atmospheric mixing ratios, it has been assumed that CO<sub>2</sub> self broadening can be neglected in favor of the much stronger foreign gas (principally nitrogen) broadening effects. A number of measurements have established that the collisional broadening mechanism (whether self or foreign) gives rise to a CO<sub>2</sub> line shape which falls off much more rapidly in the wings than can be accounted for by the Lorentz shape function [Refs.8,9]. This sub-Lorentzian

behavior is particularly evident just above the band head of the  $\text{CO}_2$  4.3 micron band. Estimates of the spectral absorption in this region based on a Lorentz lineshape are often in error by as much as a factor of 3. More recent atmospheric transmittance measurements made at sea level [Ref.10] and also from high altitude balloons [Ref.11] confirm the sub-Lorentzian behavior of line wings above the 4.3 micron band edge from about 2380 to 2420  $\text{CM}^{-1}$ .

Several explanations for the sub-Lorentzian shape in the line wings have been suggested. They range from arguments for a modified impact approximation [Ref.12] which is needed to account for the finite interaction times of molecular collisions, to the suggestion that  $\text{CO}_2\text{-N}_2$  dimer effects are important [Ref.13]. Other more involved studies have been done but will not be summarized here. See, for instance, Refs. 14 and 15.

The most useful sub-Lorentzian lineshape models to date have been empirical. The usual approach has been to modify the Lorentzian shape function with a multiparameter form factor which is obtained by fitting experimental data with trial synthetic absorption spectra. Winters, Silverman, and Benedict first used an exponential form factor which started to fall off smoothly at 5 wavenumbers from the line center and had two adjustable parameters [Ref.8]. Susskind and Mo have also used this functional form, but they adjusted it to fall off at only 0.5 wavenumbers from line center, and fitted the exponential WSB form with somewhat different parameters to accomplish the same task [Ref.16]. Burch et. al. suggested that a more complicated empirical form factor,

which also starts to fall off within one wavenumber of the line center, was needed and they proceeded to construct form factors for self and foreign gas broadening near the three CO<sub>2</sub> bands at 4.3, 2.6, and 1.4 microns [Ref.9]. Recently, Cann et. al. have restudied the problem and suggested another empirical form factor based on similar considerations [Refs.17 and 18]. The available laboratory data are not clearly inconsistent with any of these models, yet there are seemingly significant differences among the four form factors mentioned above. In particular, the size and shape of the form factor for the region within 10 wavenumbers of line center varies considerably among these models. Experience in building synthetic continuum absorption models such as these has shown that single-line features are usually blurred when the wing contributions from many lines are superposed. This fact suggests that it may not be possible to extract a unique form factor from the relatively few laboratory band-edge absorption measurements which are available.

Atmospheric measurements are also available and shed some light on the distinctions among the model predictions. Smith et. al. have compared the continuum transmission predicted by these models to balloon stratospheric solar transmission measurements [Ref.11]. Their comparison favors the models of Burch et. al. and Susskind and Mo, but some uncertainty is introduced by the presence of the pressure induced nitrogen absorption continuum, and by the fact that the strongest part of the CO<sub>2</sub> continuum above the 2397 CM-1 band head is compressed into a smaller wavenumber region at the lower stratospheric pressures where these data are taken. NRL atmospheric measurements taken over a 5.1 km path at sea level include the same nitrogen continuum, plus an uncertain water

vapor continuum contribution in the same region, and significant aerosol extinction along the optical path [Refs.10,17,18]. However, in spite of the numerous overlapping contributions, Cann et. al. do claim an improved fit to the NRL data using their own CO<sub>2</sub> form factor.

In view of the variety of model lineshapes that have been used to fit the CO<sub>2</sub> continuum, it was decided that a new two parameter exponential type form factor specifically fitted to the HIRACC algorithm would be studied for incorporation into FASCODE. We briefly review below the relevant features of the HIRACC line-by-line calculation before detailing the CO<sub>2</sub> form factor which is used. The reader is referred to Ref.2 and Ref.3 for more complete descriptions of the HIRACC algorithm.

HIRACC approximates the Voigt lineshape by a weighted sum of Lorentz and Gaussian (Doppler) lineshapes. The relative weight of each is determined by the Voigt parameter  $\zeta$ , defined in terms of the Lorentz and Doppler halfwidths according to

$$\zeta = \frac{a_L}{a_L + a_D}$$

The Lorentz function is numerically constructed by the superposition of as many as four subfunctions. A summary of the functional forms for the different domains of each subfunction is given in Table 1. Note that  $X$  is the distance from line center measured in halfwidths.

TABLE 1: FASCODE LORENTZ LINESHAPE SUBFUNCTIONS

DOMAIN	F1	F2	F3	F4	REMAINDER
$X < 4$	L-Q4	Q4-Q16	Q16-Q64	Q64-L(X=256)	L(X=256)
$4 < X < 16$	0	L-Q16	Q16-Q64	Q64-L(X=256)	L(X=256)
$16 < X < 64$	0	0	L-Q64	Q64-L(X=256)	L(X=256)
$64 < X < 256$	0	0	0	L-L(X=256)	L(X=256)
$256 < X$	0	0	0	0	L

The notable functional forms are:

L(X)	Lorentz function
Q4(X)	The quartic function whose value, slope, and curvature match the Lorentzian at X=4.
Q16(X)	The quartic function fitting L(X) at X=16.
Q64(X)	The quartic function fitting L(X) at X=64.
Q256(X)	The quartic function fitting L(X) at X=256.

The sum of the four subfunctions is the Lorentz function minus its value at X=256 for the domain within 256 halfwidths of the line center, while the sum is zero outside 256 halfwidths. The column labelled "REMAINDER" shows the "fifth" function which would be needed to complete the Lorentz shape in each domain.

The advantages of the multifunction construction have been discussed previously [Ref.2]. In particular, as the domain of each successive subfunction grows larger, the functions F1, F2, etc. grow successively smoother, so that the wavenumber grid on which each function is specified can contain approximately the same number of points. FASCODE uses these subfunctions to synthesize the single layer absorptive optical depth through line-by-line summations. Note that each subfunction has a different characteristic resolution, so that it is advantageous to carry out five separate line-by-line sums to construct five partial-absorption results (designated R1, R2, R3, R4, and ABS in the program) which are defined on successively coarser wavenumber grids. Once the five convolutions are completed, they can be merged into a single optical depth which will have the characteristic resolution typical of F1. The

manner in which the five sums are actually computed deserves some discussion. The sums R1, R2, and R3, which make up nearly all of the line contribution to band absorption, are computed line-by-line by HIRACC and its subroutines. R4 is computed by subroutine LBLF4 and its subroutines. The first four line-by-line convolutions use individual line strengths and halfwidths which are computed in each layer from the average layer pressure, temperature, and line file data at STP. The REMAINDER or "fifth" subfunction, however, is used once to precompute the total contribution of all lines to the continuum at standard temperature and pressure. When used at each layer, this stored continuum function is scaled according to

$$\text{ABS}(P,T,\text{GNU}) = \text{ABS}(P_0,T_0,\text{GNU}) [P/P_0] [T_0/T]^{.5},$$

which approximately reflects the dependence of the far wing absorption on collision frequency.

The sub-Lorentzian behavior of the CO<sub>2</sub> lineshapes is accounted for in FASCODE by multiplying both F4 and the REMAINDER by a single exponential-type form factor CHI,

$$\text{CHI}(\text{DELTA}) = \text{EXP}[- A (\text{DELTA})^B],$$

which has A and B as adjustable parameters. Delta is the distance from the line center measured in wavenumbers. Modification of the two subfunctions with this form factor produces a CO<sub>2</sub> lineshape given by

$$[ F1 + F2 + F3 ] + \text{CHI}(\text{DELTA}) [ F4 + \text{REMAINDER } ] .$$

This model is equivalent to a lineshape specified by

$$\begin{aligned} L(\text{DELTA}) - [ 1 - \text{CHI}(\text{DELTA}) ] Q64(X) & \quad \text{for} \quad X < 64 \\ \text{CHI}(\text{DELTA}) L(\text{DELTA}) & \quad X > 64 . \end{aligned}$$

This lineshape was used to construct a number of synthetic continua over the region between 2380 and 2500 CM-1. The various continua were compared to laboratory absorption measurements of WSB in order to adjust A and B for the best fit. The values  $A = 0.623$  and  $B = 0.41$  were found to give the form factor which is closest to reproducing the laboratory data. Table 2 lists this form factor which has been used by FASCODE and compares it to the others which have been discussed above. This fit was compared to others that were obtained using the simple exponential form factor (following Ref.8) which corresponds to a lineshape

$$\begin{aligned} L(\text{DELTA}) \text{EXP}[ - A (\text{DELTA}-C)^B ] & \quad \text{for} \quad \text{DELTA} > C \\ L(\text{DELTA}) & \quad \text{DELTA} < C \end{aligned}$$

with adjustable parameters A, B, and "turn-on" point C. Trial continua built using the exponential-type lineshape were found to fit the data progressively better as C was decreased from the WSB value of 5 wavenumbers to 1 wavenumber, and finally to 0.5 wavenumbers. The fits suggest that a very small value of C works best. However, one knows that the continuum absorption is quite insensitive to the lineshape within a few halfwidths of the line center. One might conclude that the "turn-on point" should not be chosen simply from considerations based on fitting

TABLE 2: COMPARISON OF VARIOUS CO<sub>2</sub> LINESHAPE FORM FACTORS

DELTA [CM-1]	FASCODE	WSB	BURCH	SUSS.,MO	CANN ET AL
2.0	0.895189	1.000000	0.414740	0.488393	0.811930
4.0	0.580513	1.000000	0.286610	0.355176	0.647770
6.0	0.283527	0.631284	0.208990	0.283801	0.507540
8.0	0.231923	0.466504	0.159790	0.236701	0.391230
10.0	0.201623	0.381189	0.127360	0.202576	0.298840
12.0	0.178058	0.324358	0.105270	0.176458	0.230360
14.0	0.159098	0.282553	0.089794	0.155722	0.185820
16.0	0.143463	0.250046	0.078712	0.138817	0.165190
18.0	0.130322	0.223839	0.070627	0.124757	0.156520
20.0	0.119111	0.202165	0.064643	0.112875	0.148310
22.0	0.109428	0.183890	0.060164	0.102705	0.140540
24.0	0.100979	0.168248	0.056780	0.093905	0.133190
26.0	0.093543	0.154697	0.054202	0.086222	0.126240
28.0	0.086949	0.142838	0.052221	0.079462	0.119660
30.0	0.081065	0.132373	0.050681	0.073474	0.113440
32.0	0.075783	0.123070	0.049462	0.068138	0.107570
34.0	0.071019	0.114748	0.048472	0.063358	0.102020
36.0	0.066702	0.107264	0.047638	0.059056	0.096774
38.0	0.062774	0.100500	0.046900	0.055168	0.091822
40.0	0.059188	0.094360	0.046213	0.051640	0.087148
42.0	0.055901	0.088766	0.045538	0.048429	0.082736
44.0	0.052881	0.083650	0.044848	0.045495	0.078572
46.0	0.050098	0.078957	0.044120	0.042808	0.074644
48.0	0.047526	0.074639	0.043340	0.040340	0.070939
50.0	0.045144	0.070656	0.042496	0.038068	0.067444
52.0	0.042933	0.066972	0.041585	0.035971	0.064148
54.0	0.040877	0.063558	0.040605	0.034031	0.061040
56.0	0.038960	0.060387	0.039558	0.032233	0.058110
58.0	0.037170	0.057435	0.038451	0.030563	0.055347
60.0	0.035496	0.054683	0.037290	0.029011	0.052743
62.0	0.033928	0.052113	0.036084	0.027564	0.050287
64.0	0.032457	0.049709	0.034844	0.026213	0.047972
66.0	0.031074	0.047456	0.033580	0.024951	0.045789
68.0	0.029774	0.045342	0.032302	0.023770	0.043730
70.0	0.028549	0.043355	0.031021	0.022663	0.041789
72.0	0.027394	0.041487	0.029746	0.021625	0.039958
74.0	0.026303	0.039727	0.028486	0.020649	0.038230
76.0	0.025271	0.038067	0.027248	0.019731	0.036599
78.0	0.024295	0.036500	0.026040	0.018866	0.035059
80.0	0.023371	0.035019	0.024866	0.018052	0.033605
82.0	0.022495	0.033618	0.023732	0.017283	0.032231
84.0	0.021663	0.032292	0.022640	0.016557	0.030933
86.0	0.020873	0.031035	0.021594	0.015870	0.029705
88.0	0.020122	0.029842	0.020595	0.015221	0.028543
90.0	0.019407	0.028710	0.019643	0.014606	0.027443

TABLE 2 (CONT.):

DELTA [CM-1]	FASCODE	WSB	BURCH	SUSS.,MO	CANN ET AL
92.0	0.018727	0.027634	0.018739	0.014023	0.026401
94.0	0.018079	0.026612	0.017883	0.013470	0.025413
96.0	0.017461	0.025638	0.017074	0.012945	0.024477
98.0	0.016871	0.024711	0.016310	0.012446	0.023587
100.0	0.016308	0.023828	0.015591	0.011972	0.022742
102.0	0.015770	0.022986	0.014913	0.011521	0.021939
104.0	0.015255	0.022182	0.014276	0.011092	0.021175
106.0	0.014763	0.021415	0.013677	0.010683	0.020447
108.0	0.014292	0.020682	0.013114	0.010294	0.019754
110.0	0.013841	0.019981	0.012584	0.009922	0.019092
112.0	0.013408	0.019311	0.012087	0.009568	0.018460
114.0	0.012994	0.018670	0.011619	0.009229	0.017857
116.0	0.012596	0.018056	0.011179	0.008906	0.017280
118.0	0.012214	0.017468	0.010765	0.008597	0.016728
120.0	0.011848	0.016905	0.010374	0.008302	0.016199
122.0	0.011496	0.016364	0.010005	0.008019	0.015692
124.0	0.011158	0.015846	0.009656	0.007749	0.015206
126.0	0.010832	0.015348	0.009326	0.007490	0.014739
128.0	0.010519	0.014871	0.009012	0.007241	0.014291
130.0	0.010218	0.014412	0.008714	0.007003	0.013861
132.0	0.009928	0.013971	0.008431	0.006775	0.013447
134.0	0.009649	0.013547	0.008160	0.006557	0.013049
136.0	0.009380	0.013139	0.007901	0.006347	0.012665
138.0	0.009121	0.012747	0.007653	0.006145	0.012297
140.0	0.008871	0.012370	0.007414	0.005951	0.011941
142.0	0.008630	0.012006	0.007185	0.005765	0.011599
144.0	0.008397	0.011657	0.006964	0.005587	0.011270
146.0	0.008172	0.011319	0.006750	0.005415	0.010953
148.0	0.007956	0.010994	0.006543	0.005249	0.010647
150.0	0.007746	0.010681	0.006343	0.005090	0.010353
152.0	0.007544	0.010379	0.006149	0.004937	0.010070
154.0	0.007348	0.010087	0.005960	0.004790	0.009797
156.0	0.007159	0.009806	0.005776	0.004648	0.009535
158.0	0.006976	0.009535	0.005598	0.004511	0.009283
160.0	0.006800	0.009273	0.005424	0.004379	0.009040
162.0	0.006629	0.009019	0.005255	0.004252	0.008807
164.0	0.006463	0.008775	0.005090	0.004129	0.008584
166.0	0.006303	0.008538	0.004929	0.004011	0.008370
168.0	0.006147	0.008310	0.004773	0.003897	0.008164
170.0	0.005997	0.008089	0.004620	0.003787	0.007967
172.0	0.005851	0.007875	0.004472	0.003681	0.007779
174.0	0.005710	0.007668	0.004329	0.003578	0.007599
176.0	0.005573	0.007468	0.004189	0.003479	0.007428
178.0	0.005441	0.007275	0.004053	0.003383	0.007265
180.0	0.005312	0.007087	0.003922	0.003291	0.007109
182.0	0.005187	0.006906	0.003795	0.003201	0.006961
184.0	0.005066	0.006730	0.003672	0.003115	0.006821
186.0	0.004948	0.006560	0.003553	0.003031	0.006689
188.0	0.004834	0.006395	0.003439	0.002950	0.006563

TABLE 2 (CONT.):

DELTA [CM-1]	FASCODE	WSB	BURCH	SUSS.,MO	CANN ET AL
190.0	0.004723	0.006235	0.003329	0.002872	0.006445
192.0	0.004616	0.006080	0.003223	0.002796	0.006334
194.0	0.004511	0.005930	0.003121	0.002723	0.006229
196.0	0.004410	0.005784	0.003024	0.002652	0.006131
198.0	0.004311	0.005642	0.002930	0.002583	0.006040
200.0	0.004215	0.005505	0.002841	0.002517	0.005954
202.0	0.004122	0.005372	0.002755	0.002452	0.005875
204.0	0.004032	0.005243	0.002674	0.002390	0.005801
206.0	0.003943	0.005118	0.002596	0.002329	0.005733
208.0	0.003858	0.004996	0.002522	0.002270	0.005670
210.0	0.003774	0.004878	0.002452	0.002213	0.005613
212.0	0.003693	0.004763	0.002385	0.002158	0.005560
214.0	0.003614	0.004651	0.002322	0.002105	0.005513
216.0	0.003537	0.004543	0.002262	0.002053	0.005469
218.0	0.003463	0.004437	0.002205	0.002002	0.005430
220.0	0.003390	0.004335	0.002151	0.001953	0.005395
222.0	0.003319	0.004236	0.002099	0.001906	0.005364
224.0	0.003250	0.004139	0.002051	0.001860	0.005336
226.0	0.003183	0.004045	0.002005	0.001815	0.005311
228.0	0.003117	0.003953	0.001961	0.001772	0.005290
230.0	0.003053	0.003864	0.001919	0.001729	0.005271
232.0	0.002991	0.003778	0.001880	0.001688	0.005255
234.0	0.002930	0.003693	0.001842	0.001649	0.005241
236.0	0.002871	0.003611	0.001806	0.001610	0.005229
238.0	0.002813	0.003532	0.001771	0.001572	0.005219
240.0	0.002757	0.003454	0.001738	0.001536	0.005210
242.0	0.002702	0.003378	0.001706	0.001500	0.005203
244.0	0.002649	0.003305	0.001675	0.001466	0.005197
246.0	0.002597	0.003233	0.001645	0.001432	0.005192
248.0	0.002546	0.003163	0.001615	0.001399	0.005188
250.0	0.002496	0.003095	0.001586	0.001367	0.005184

the continuum, since the small value of  $C$  may be more an artifact of forcing the form factor to be of the exponential type than it is a real phenomenon. Additionally, one risks altering the integrated line-strength if the "turn-on point" is too close to the line center. With the use of a value of  $C \ll 1$ , it could become necessary to renormalize the line strengths in order to handle this difficulty consistently.

One advantage of the FASCODE  $\text{CO}_2$  lineshape is that the problem of specifying a turn-on point for sub-Lorentzian behavior has been avoided. The key test of this lineshape is whether it can produce a continuum absorption curve which compares favorably to the other exponential-type fits. We have found the FASCODE shape to fit the WSB data slightly better than the best simple exponential form factor with  $C = 0.5$ . The difference is slight, but the FASCODE lineshape model does appear to be more than adequate to fit the data. A comparison was also made with the simulated  $\text{CO}_2$  continuum transmittance for a 5.1 km atmospheric path reported in Ref.18. The FASCODE predictions are displayed in Fig.1 as points on the top curve of Roney et. al. The comparison reflects a difference of only 1-2 percent between the two models.

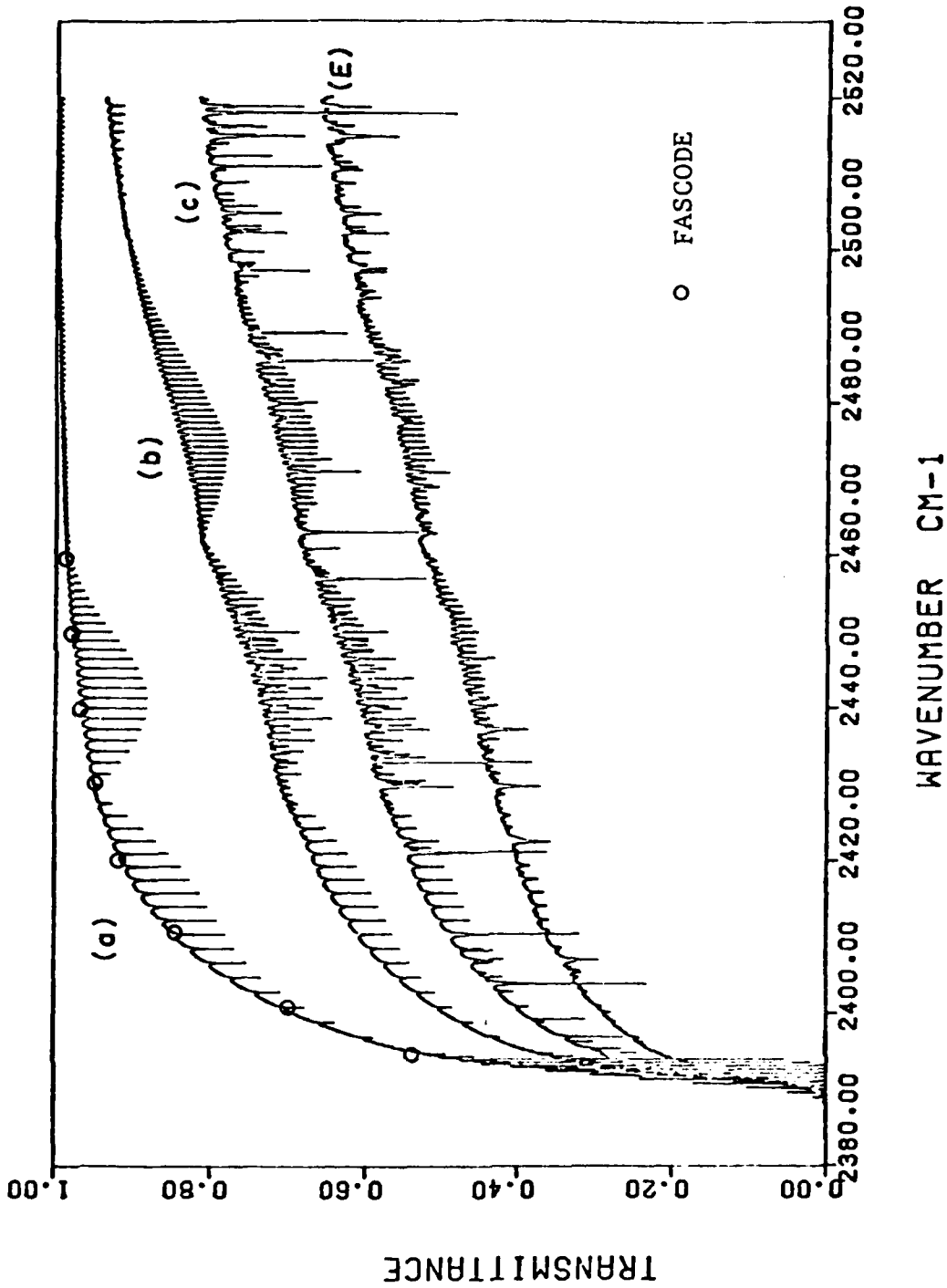


Figure 1. Comparison of sample FASCODE CO<sub>2</sub> transmittances to other simulations of (E) NRL Field Spectrum S154. Transmittance curves for (a) CO<sub>2</sub> only, (b) N<sub>2</sub> continuum and N<sub>2</sub>O lines added, and (c) water vapor continuum added, are taken from Ref. 18.

### 3. NON-LTE RADIANCE AND TRANSMITTANCE CALCULATIONS

In this section we review the monochromatic radiative transfer properties of an absorbing gaseous medium which may not be in local thermodynamic equilibrium. Those assumptions and relationships which are valid only under LTE circumstances are distinguished from the quite general aspects of radiative transfer. The transfer equation describes the influence which the atmospheric environment (the optical medium) has on the radiation field, and this is the problem which FASCODE has been designed to address. The radiation may also, to varying degrees, affect the state of the gas, both as a driving force that stimulates molecular excitations, and as a vehicle for energy exchange and relaxation within the medium. The largest single effect of solar radiation on the earth's atmosphere is simple heating. However, selective molecular excitation and photochemical mechanisms combined with the slower relaxation rates of the upper atmosphere also tend to drive the medium away from a state of thermal equilibrium.

High altitude limb radiance measurements have confirmed that certain species, notably water vapor, carbon dioxide, ozone, and nitric oxide, may be found in non-LTE states above about 40 - 60 km altitude (even lower for NO) [Ref.6]. In the upper atmosphere, it is necessary to account for these non-thermodynamic states of the optical medium if its radiative properties are to be properly modelled. At lower altitudes, the LTE assumption is generally valid, but the local temperature

is found to change considerably from the boundary mixing layer to the upper stratosphere.

FASCODE calculates only the radiative intensity at a chosen altitude for a particular direction of observation. The code therefore implicitly decouples the problem of solving for these intensities from the problem of finding the state of the medium itself. The properties of an LTE medium which are needed to perform the calculation are not computed or modelled by FASCODE, but are accessible in the form of stored atmospheric profiles (temperature, pressure, molecular densities) plus an off-line file containing molecular line data [Ref.19]. The non-LTE problem requires a more detailed description of the propagating medium, so that some generalization of the standard profiles is needed for this case.

The problem can be described by the quite general governing equation for the monochromatic radiative intensity  $I_\nu$ ,

$$\frac{dI_\nu}{ds} = K_\nu I_\nu + R_\nu$$

The parameter  $s$  is taken to be a length parameter along a (possibly curved) line-of-sight through the atmosphere. (This can be converted to a molecular amount per unit area or gas column density.) The local monochromatic volumetric extinction is  $K_\nu$ , and  $R_\nu$  is the source term giving the radiance per unit length. It is important to note that both  $K_\nu$  and  $R_\nu$  are linear functions of the densities of each IR-active

gas and aerosol constituent. That is, the contribution to both quantities can be added line-by-line, molecule-by-molecule, aerosol-by-aerosol, etc.

The basic problem is one of calculating the contribution to both  $K_v$  and  $R_v$  of each molecular absorption/emission line. In order to illustrate the processes involved, we focus on a single typical vibrational-rotational transition (line) between an upper state  $u$  and lower state  $l$ . In terms of the Einstein coefficients  $B_{lu}$ ,  $B_{ul}$ , and  $A_{ul}$ , for absorption, stimulated, and spontaneous emission, respectively, the volumetric absorption and radiance for this transition are

$$K_v = \frac{h\nu}{4\pi} (B_{lu} n_l \phi_v - B_{ul} n_u \psi_v)$$

and

$$R_v = \frac{h\nu}{4\pi} A_{ul} n_u \chi_v$$

with  $\phi_v$ ,  $\psi_v$ , and  $\chi_v$  representing normalized lineshape functions of the frequency difference ( $\nu - \nu_0$ ).  $n_l$  and  $n_u$  are the lower and upper single V-R state populations.

The Einstein coefficients are a set of rate coefficients which are intrinsic to this transition, but which are not all independent. This fact is generally true, but most easily demonstrated by looking to equilibrium considerations. At equilibrium, the radiation field within a large homogenous medium of temperature  $T$  will be isotropic and have

an intensity distributed according to the Planck function

$$B_\nu(T) = \frac{2 h \nu^3}{c^2 (e^{h\nu/kT} - 1)}$$

Additionally, the populations of the upper and lower states have the ratio

$$\frac{g_l n_u^e}{g_u n_l^e} = \exp(-h\nu_0/kT)$$

which defines the Boltzmann distribution for the temperature  $T$ . The  $g$ 's are single state degeneracy factors. The superscript "e" is used throughout to denote the equilibrium state. Since the intensity doesn't change with position in this case, the equation of transfer reduces to

$$R_\nu = K_\nu B_\nu(T)$$

which implies that

$$A_{ul} n_u = (B_{lu} n_l - B_{ul} n_u) B_\nu(T)$$

The symmetry of the quantum matrix elements also requires that

$g_u B_{ul} = g_l B_{lu}$ , so that the three Einstein coefficients can be expressed in terms of a single rate coefficient  $\bar{B}$  according to

$$B_{lu} = g_u \bar{B}$$

$$B_{ul} = g_l \bar{B}$$

$$A_{ul} = \frac{2h\nu^3}{c^2} g_l \bar{B}$$

Note that the three lineshapes are also not independent. Several assumptions can be made regarding these lineshapes. Both the collisional and Doppler line broadening mechanisms are dependent on bulk thermodynamic properties ( P and T ) and not on "internal" degrees of freedom (such as the V-R state populations  $n_l$  and  $n_u$  ), so the lineshapes are usually assumed to have the LTE form even under non-LTE conditions.

The assumption is made here that the (net) absorption lineshape is the same under daylight conditions as it is under LTE conditions. This is equivalent to assuming that absorption and stimulated emission have the same lineshape, i.e.,  $\psi_\nu = \phi_\nu$ . The relationship which completes the set consistently in the equilibrium limit is

$$\chi_\nu = \frac{\exp(h\nu_0/kT)-1}{\exp(h\nu/kT)-1} \phi_\nu$$

Other arguments which lead to a different set of lineshape relations have been made (see Ref.20), but either set of relations can only be regarded as speculative with the limited knowledge of non-LTE lineshapes to date. It should be noted that, except for the microwave region, the effects of these lineshape differences are quite small in comparison to those of the uncertainties in the non-LTE line strengths. The differences are insignificant for the narrow Doppler lines at high altitude.

With the above assumption, the single-line volumetric absorption and radiance is given by

$$K_{\nu} = \frac{h\nu}{4\pi} \bar{B}(g_u n_l - g_l n_u) \phi_{\nu}$$

and

$$R_{\nu} = \frac{h^2 \nu^4}{2\pi c^2} \bar{B} g_l n_u \chi_{\nu}$$

This result is a general one for a two-level system. The lineshapes are functions of the bulk thermodynamic quantities such as pressure, temperature, and gas densities. The populations are given by the Boltzman distribution only under conditions of local thermodynamic equilibrium. In the presense of a strong radiation field, or under conditions where relaxation rates are small, the upper and lower state populations may bear no special relationship to each other. Therefore, the absorption and radiance owing to any single transition (and to all transitions of all molecules) are not simply related for a non-LTE atmosphere, and more specifically, the radiance from such an optically thick atmosphere will not be given by the Planck function.

In the upper atmosphere, relaxation rates for the different excitation modes of various molecules are found to vary considerably. Rotational degrees of freedom generally relax much more rapidly to a state of thermal equilibrium than do vibrational modes. The work of Degges and Smith [Ref.6] make use of this fact to construct a high altitude model which calculates vibrational state populations, while assuming that the rotational state populations are thermally distributed within each vibrational state according to the Boltzman distribution for

the translational (bulk) temperature. Thus, this model employs a single kinetic temperature, which is a function of altitude, plus a set of vibrational state population variables.

These vibrational population variables can be used to relate the non-LTE single-line absorption and radiance to the same quantities calculated for an atmosphere in equilibrium at the kinetic temperature. The relationship between equilibrium and non-equilibrium radiative properties for a single line can be summarized by

$$K_v = \frac{g_u n_l - g_l n_u}{g_u n_l^e - g_l n_u^e} K_v^e$$

and

$$R_v = \frac{n_u}{n_u^e} R_v^e$$

which can also be written in terms of the Planck function as

$$R_v = \frac{n_u}{n_u^e} B_v(T) K_v^e$$

These relations provide for the calculation of absorption and radiance spectral functions using two separate line-by-line sums. (The two sums would be related by the Planck function in the equilibrium limit.) The non-LTE algorithm of FASCODE calculates  $K_v$  directly, but the radiance is computed from a line-by-line sum of the quantity  $C_v$  defined by

$$C_v = K_v - \frac{R_v}{B_v(T)}$$

which can be viewed as representing that part of the non-LTE absorption which is not returned to the radiation field as thermal emission. Any two of the spectral functions  $K_v$ ,  $R_v$ , and  $C_v$  can easily be used to obtain the third, so the choice of summing  $C_v$  rather than  $R_v$  is made for computational reasons.  $C_v$  can be seen to vanish in the equilibrium limit, and furthermore, in an atmosphere of mixed gases, only transitions of those gases which are not in thermal equilibrium will contribute to  $C_v$ . This property is used by FASCODE to shorten the second line-by-line sum where possible.

To compute the absorption and radiance for optical path segments in the upper atmosphere, FASCODE employs the vibrational population model of Degges and Smith [Ref.6]. Each IR line corresponds to a transition between two molecular vibrational states. The identification of these two states is made by BCDNLTE, a separate routine modelled after BCDMRG [Ref.2], which prepares a blocked line data file for FASCODE. The population of each vibrational state is referenced to its equilibrium value, calculated at the kinetic temperature  $T$ . The ratios of non-LTE vibrational populations to their reference values are given by the enhancement (or depletion) ratios

$$r_l = \frac{n_l}{n_l^e} \quad \text{and} \quad r_u = \frac{n_u}{n_u^e}$$

The fact that rotational sub-states are thermally distributed has been used to relate the vibrational state population ratios directly to single V-R state population ratios. That is, rotational partition functions and Boltzman factors produce a factor of unity in the V-R ratios. The single-line contributions to  $K_v$  and  $C_v$  can be expressed simply in terms of these ratios according to

$$K_v = \left[ \frac{r_l - r_u \Delta}{1 - \Delta} \right] K_v^e$$

and

$$C_v = \left[ \frac{r_l - r_u}{1 - \Delta} \right] K_v^e$$

where  $\Delta$  is the Boltzman factor,

$$\Delta = \frac{g_l n_u^e}{g_u n_l^e} = \exp(-h\nu_0/kT)$$

Thus, the two factors in the brackets can be taken to be effective line-strength correction factors for these two "effective absorption" line-by-line calculations.

To summarize, if "i" denotes a single absorption line of a particular molecular species, the two functions  $K_v$  and  $C_v$  are obtained by performing the two sums

$$K_v = \sum_i K_v^i \quad \text{and} \quad C_v = \sum_i C_v^i$$

which are taken over all lines of all molecules in the case of  $K_v$ , and over all lines connecting non-equilibrium vibrational populations in the case of  $C_v$ . The single-line functions are given by the previous equations. The solution of the radiative transfer equation for a path of length  $L$  through a homogeneous layer, including self-absorption of emitted radiation, is calculated directly as

$$I_v = I_v^0 \exp(-K_v L) + B_v \left(1 - \frac{C_v}{K_v}\right) (1 - e^{-K_v L})$$

The FASCODE subroutines which perform the calculations discussed above are described in the next section.

Sample calculations have been made using this high resolution non-LTE model. Figure 2 shows the enhancement of the predicted radiance by non-equilibrium vibrational populations, which would be seen by an observer looking along a 500 km horizontal path at an altitude of 100 km. The comparison of LTE and non-LTE calculations is made for a spectral region within the 4.3 micron band of  $\text{CO}_2$ . This band and others often show radiance enhancements by several orders of magnitude over what could be expected of a gas at thermal equilibrium.

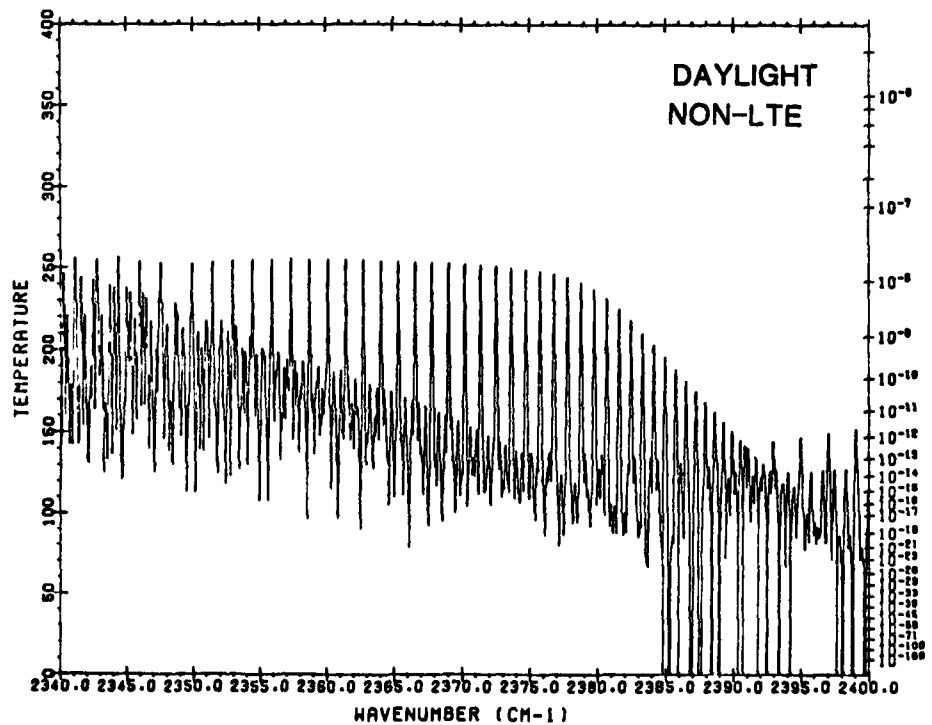
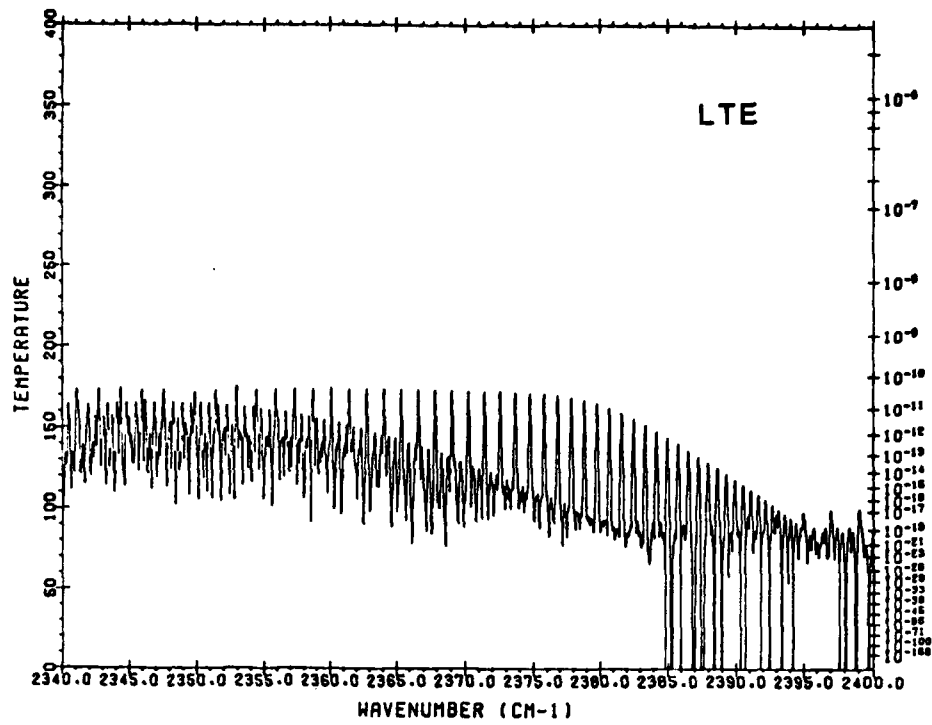


Figure 2. Radiance in Units of Equivalent Blackbody Temperature for a 500 km Path at 100 km Altitude Assuming LTE and Non-LTE Vibrational Populations

#### 4. LINESHAPE CONTROL FEATURES AND PROGRAM STRUCTURE CHANGES

The three control parameters IHIRAC, ILBLF4, and ICNTNM, which appear on CARD 2 of the input file, govern which of the Lorentz subfunctions are used. The various combinations are enumerated below:

IHIRAC=1 allows the line-by-line summation algorithm to be used with the three subfunctions F1, F2, and F3 which cover the region within 64 halfwidths of line center (for all molecules).

ILBLF4=1 adds the fourth subfunction F4 (if IHIRAC=1) to the first three subfunctions. F4 is modified by the exponential factor CHI in the case of CO<sub>2</sub> only.

ICNTNM=1 adds the scaled "fifth" or REMAINDER continuum subfunction for CO<sub>2</sub>, N<sub>2</sub>, and water vapor.

Table 3 shows the fourth and "fifth" subfunction program routine structure. The asterisk indicates where FASCOD2 routines have been changed significantly from earlier versions. Program changes related to the sub-Lorentzian CO<sub>2</sub> lineshape have been confined largely to the routines SHRINK, CONVF4, and to the CO<sub>2</sub> continuum function stored in FRNCO2.

FASCODE routines which are specifically used to calculate non-LTE transmittance and radiance are listed in Table 4. The non-LTE calculation uses a straightforward extension of the HIRAC line-by-line algorithm, which is made to perform two line-by-line calculations simultaneously. An entirely new program branch (bearing the interim name HIRACQ) has been constructed to do the non-LTE calculation. The new branch routines HIRACQ, CNVFNQ, and PANELQ are the non-LTE analogs of

TABLE 3: ROUTINES USED TO PRODUCE THE CO<sub>2</sub> LINESHAPE

LBLF4 ROUTINES

LBLF4	Fourth function driver. Scales line strengths by column density amounts and temperature correction factors. Calculates P and T adjusted halfwidths ALFAD and ALFAV. Modifies R4 by radiation field term and returns R4 to LAYER for later merger with ABSRB, R3, R2, and R1.
VOICON	Computes the Voigt profile factor AVRAT(IZETA)
MOLEC	Computes line strength (SCOR) and Lorentz halfwidth (ALFCOR) correction factors from P and T. Also calculates the Doppler halfwidth (ALFD1) at GNU=1.
RDLIN4	Up to 1250 lines are loaded into the arrays GNU(I), S(I), ALFAL(I), ALFAD(I) and MOL(I). * The Non-LTE vibrational transition index is stripped from the MOL array. BUFIN is called to read blocked line data from TAPE3.
SHRINK	Merges nearby lines together to form fewer effective lines. * CO <sub>2</sub> and non-CO <sub>2</sub> lines are 'lumped' separately. Returns the new line data: GNU(J)       strength-weighted average frequency S(J)         summed line strength for merged lines ALFAL(J)     strength-weighted Lorentz halfwidth ALFAD(J)     strength-weighted Doppler halfwidth * MOL(J)     molecular ID =0 for non-CO <sub>2</sub> lines =2 for CO <sub>2</sub> lines
CONVF4	Performs line-by-line fourth function sum to produce the R4 array. * Uses a Lorentz subfunction F4 which is modified by the exponential form factor CHI for CO <sub>2</sub> lines only.
RADFN	Returns the value of the radiation field term.

TABLE 3 (CONT.):

CONTINUUM ROUTINES

CONTNM	Scales/interpolates stored continuum data and loads the array ABSRB.
SLF296	Stored self-broadened H <sub>2</sub> O continuum for T=296 K.
SLF260	Stored self-broadened H <sub>2</sub> O continuum for T=260 K.
FRN296	Stored foreign-broadened H <sub>2</sub> O continuum for T=296 K.
FRNCO2	* Stored foreign-broadened CO <sub>2</sub> continuum for T=296 K. Includes the sub-Lorentz 'REMAINDER' subfunction.
CONT	Called by HIRAC to merge ABSRB and R4 into R3.

HIRAC1, CNVFNV, and PANEL. The subroutine STRTHS is used by HIRACQ to compute the two "effective strengths" for each line which is enhanced or diminished by the non-thermal vibrational populations. The vibrational populations of H<sub>2</sub>O, CO<sub>2</sub>, O<sub>3</sub>, and NO as functions of altitude are taken directly from the appropriate output file of the Degges high altitude computer model. The populations are read from this file and used to calculate the vibrational state population enhancement ratios by the FASCODE subroutine RDPOPS. The ratios are stored for use by STRTHS. The actual single-layer radiance calculation is performed by EMIN, which has been modified to calculate  $R_v$  from the HIRACQ functions  $K_v$  and  $C_v$ .

A new offline program called BCDNLTE prepares the blocked line data file for use by FASCODE in doing non-LTE calculations. In addition to formatting the line data (frequency, strength, halfwidth, lower state energy, and molecular ID), this program sorts the lines into equilibrium and non-equilibrium transitions, and then adds two vibrational state code numbers to the molecular ID. Code numbers are presently chosen to be compatible with the Degges model, but could be altered to allow use of other non-LTE gas models in the future.

TABLE 4: NON-LTE ROUTINES

BCDNLTE	Prepares a blocked line file for use in the non-LTE calculation. Vibrational state labels are coded and added to the molecular ID for each non-equilibrium line.
RDPOPS	Reads the file containing non-LTE population data. Calculates population enhancement ratios.
HIRACQ	Performs two separate line-by-line calculations.
STRTHS	Computes the effective line strength for absorption and for the second function C. Returns these two strengths to HIRACQ for each line.
CONVFNQ	Constructs the arrays (R1,R2,R3; RR1,RR2,RR3) which are needed for the two line-by-line sums.
PANELQ	Merges the two separate sets of subfunctions and writes the spectral functions K and C to a temporary file.
EMIN	Calculates the single layer radiance and transmittance from the spectral functions K and C.

## 5. SUMMARY

This and the previous report [Ref.1] complete the description and documentation of the following four tasks: 1) using a new geometry routine in FASCOD2, 2) incorporating aerosol absorption and scattering for the atmospheric models of LOWTRAN 5, 3) modelling the far wings of lines to characterize continuum absorption near the CO<sub>2</sub> band head, and 4) modifying the code to allow for non-LTE effects at the higher altitudes. The one remaining task is that of constructing a scheme which enables one to operate the code with as few atmospheric layers as possible while maintaining reasonable accuracy. Such work is still underway as presented in Ref.1.

In addition to the major tasks listed above, certain operational problems with the code have yet to be addressed. The version of FASCOD2 that is the product of incorporating the geometry and atmospheric data changes is not the AFGL code designated FASCOD1B. Therefore, features of both codes must yet be combined to produce the new working version to be designated FASCOD2. In addition, the now modified FASCOD2 requires somewhat more central memory during execution. This problem may be overcome with a careful study of space usage so as to allow segmented on-line execution of the code. The final code will be executed in each of its modes to verify that all subprograms and modifications have been integrated correctly.

## REFERENCES

1. Ridgway, W.L., Moose, R.A., and Cogley, A.C., "Atmospheric Transmittance/Radiance Computer Code FASCOD2", AFGL-TR-80-0250 (1980).
2. Smith, H.J.P., Dube, D.J., Gardner, M.E., Clough, S.A., Kneizys, F.X. and Rothman, L.S., "FASCODE - Fast Atmospheric Signature Code (Spectral Transmittance and Radiance)", AFGL-TR-78-0081 (1978).
3. Clough, S.A. and Kneizys, F.X., "FASCOD1B", private communication (1981).
4. Gallery, W.O., Kneizys, F.X., and Clough, S.A., "ATMPATH - Computer Code ATMOSPHERIC PATH", private communication (1979).
5. Kneizys, F.X., Shettle, E.P., Gallery, W.O., Chetwynd, J.H., Abreu, L.W., Selby, J.E.A., Fenn, R.W., and McClatchy, R.A., "Atmospheric Transmittance/Radiance: Computer Code LOWTRAN 5", AFGL-TR-80-0067 (1980).
6. Degges, T.C. and Smith, H.J.P., "A High Altitude Infrared Radiance Model", AFGL-TR-77-0271 (1977).
7. Clough, S.A., Kneizys, F.X., and Chetwynd, J.H., "Algorithm for the Calculation of Absorption Coefficient-Pressure Broadened Molecular Transitions", AFCRL-TR-77-0164 (1977).
8. Winters, B.H., Silverman, S., and Benedict, W.S., J.Q.S.R.T. 4, 527 (1964).
9. Burch, D.E., Gryvnak, D.A., Patty, R.R., and Bartky, C.E., J. Opt. Soc. Am. 59, 267 (1969).
10. K.M. Haight, "High Resolution Atmospheric Transmission Spectra from 5 to 3  $\mu\text{M}$ ", NRL Report 8297, Naval Research Laboratory, Washington, D.C. (1979).
11. Smith, M.A.H., Russell III, J.M., and Park, J.H., "Measurements of Continuum Absorption near 2400  $\text{cm}^{-1}$  in the Lower Stratosphere", Preprint Volume, Fourth Conference on Atmospheric Radiation, Toronto, Canada, American Meteorological Society, Boston, Mass. (1981).
12. Clough, S.A. and Kneizys, F.X., private communication (1980).
13. Bernstein, L.S., Robertson, D.C., Conant, J.A., and Sandford, B.P., App. Opt. 18, 2454 (1979).

REFERENCES (CONT.)

14. Ben-Aryeh, Y., Weissman, E., and Postan, A., J.Q.S.R.T. 18, 597 (1977).
15. Postan, A., Weissman, E., and Ben-Aryeh, Y., J.Q.S.R.T. 18, 617 (1977).
16. Susskind, J. and Mo, I., Preprint Volume, Third Conference on Atmospheric Radiation, Davis, California, American Meteorological Society, Boston, Mass. (1978).
17. Cann, M.W.P., Nicholls, R.W., Roney, P.L., Findlay, F.D., and Blanchard, A., Technical Digest, Topical Meeting on Spectroscopy in Support of Atmospheric Measurements, Sarasota, Florida (1980).
18. Roney, P.L., Findlay, F.D., Blanchard, A., Cann, M.W.P., and Nicholls, R.W., Opt. Lett. 6, 151 (1981).
19. McClatchey, R.A., Benedict, W.S., Clough, S.A., Burch, D.E., Calfee, R.F., Fox, K., Rothman, L.S., and Garing, J.S., "AFCRL Atmospheric Absorption Line Parameters Compilation", AFCRL-TR-73-0096 (1977).
20. Gilles, S.E., "Flow with Coupled Radiative and Vibrational Nonequilibrium in a Diatomic Gas", Air Force Office of Scientific Research Report 68-1895 (1968).

**ILMED**  
**8**